



ELSEVIER

Available online at [www.sciencedirect.com](http://www.sciencedirect.com)

SCIENCE @ DIRECT®

Nuclear Instruments and Methods in Physics Research A 544 (2005) 553–564

NUCLEAR  
INSTRUMENTS  
& METHODS  
IN PHYSICS  
RESEARCH  
Section A

[www.elsevier.com/locate/nima](http://www.elsevier.com/locate/nima)

# ZnWO<sub>4</sub> crystals as detectors for 2β decay and dark matter experiments

F.A. Danevich<sup>\*</sup>, V.V. Kobychiev, S.S. Nagorny, D.V. Poda, V.I. Tretyak,  
S.S. Yurchenko, Yu.G. Zdesenko<sup>\*</sup>

*Institute for Nuclear Research, Prospekt Nauki 47, MSP 03680 Kiev, Ukraine*

Received 8 November 2004; accepted 4 January 2005  
Available online 11 March 2005

## Abstract

Energy resolution,  $\alpha/\beta$  ratio, and the pulse shape discrimination ability of the ZnWO<sub>4</sub> crystal scintillators were studied. The radioactive contamination of a ZnWO<sub>4</sub> crystal was investigated in the Solotvina Underground Laboratory. Possibilities to apply ZnWO<sub>4</sub> crystals for the dark matter and double beta decay searches are discussed. New improved half-life limits on double beta decay in zinc isotopes were established, in particular, for  $\epsilon\beta^+$  decay of <sup>64</sup>Zn as:  $T_{1/2}^{2\nu} \geq 8.9 \times 10^{18}$  years and  $T_{1/2}^{0\nu} \geq 3.6 \times 10^{18}$  years, both at 68% CL.

© 2005 Elsevier B.V. All rights reserved.

PACS: 29.40.Mc; 23.40.–s; 95.35.+d

Keywords: ZnWO<sub>4</sub> crystal scintillators; Double beta decay; Dark matter

## 1. Introduction

Observation of the neutrinoless (0ν) double beta (2β) decay and/or dark matter particles would be extraordinary events for the modern physics. It is because both the phenomena are related to the new physical effects beyond the Standard Model of the particle theory.

The great interest to the 0ν2β decay searches [1–4] have arisen from the recent evidence of neutrino oscillations, strongly suggesting that neutrinos have nonzero mass. While oscillation experiments are sensitive to the neutrinos mass difference, only the measured 0ν2β decay rate could establish the Majorana nature of the neutrino and give the absolute scale of the effective neutrino mass.

Several sensitivity studies of the 2β decay processes were performed using low background crystal scintillators, which contain various candidate nuclei: <sup>40</sup>Ca [5], <sup>48</sup>Ca [6,7], <sup>106</sup>Cd [8,9], <sup>108</sup>Cd,

<sup>\*</sup>Corresponding author. Tel: +380 44 525 1111;  
fax: +380 44 525 4463.

E-mail address: [danevich@kinr.kiev.ua](mailto:danevich@kinr.kiev.ua) (F.A. Danevich).

<sup>\*</sup>Deceased.

$^{114}\text{Cd}$  and  $^{116}\text{Cd}$  [9],  $^{136}\text{Ce}$  and  $^{138}\text{Ce}$  [10],  $^{160}\text{Gd}$  [11],  $^{180}\text{W}$  and  $^{186}\text{W}$  [12,9]. For instance, in the experiment [9] with the cadmium tungstate ( $\text{CdWO}_4$ ) scintillators enriched in  $^{116}\text{Cd}$  the very low counting rate of 0.04 counts/(year keV kg) was reached in the energy window 2.5–3.2 MeV. The half-life limit on  $0\nu 2\beta$  decay of  $^{116}\text{Cd}$  was set as  $T_{1/2}^{0\nu 2\beta} \geq 1.7 \times 10^{23}$  years at 90% CL, which leads to one of the strongest restriction on the effective Majorana neutrino mass  $\langle m_\nu \rangle \leq 1.7$  eV.

There are strong evidence for a large amount of dark matter in the Universe (matter which reveals itself only through gravitational interaction). Weakly interacting massive particles (WIMP)—in particular neutralino, predicted by the Minimal Supersymmetric extensions of the Standard Model—are considered as one of the most acceptable component of the dark matter [13]. These particles can be detected due to their scattering on nuclei producing low energy nuclear recoils. Extremely low counting rate and small energy of recoil nuclei are expected in experiments to search for the WIMP. Therefore, the experiments for direct WIMP search require extremely low level of background (less than several events per kilogram per day per keV) with very low energy threshold (less than tens keV).

Direct methods of WIMP detection are based on registration of ionization or/and excitation of recoil nucleus in the material of the detector itself. At present, most sensitive experiments apply different detectors for WIMP search: Ge semiconductor detectors [14–16], bolometers [17,18], scintillation detectors [19–25]. An interesting possibility to reject background caused by electrons provides cryogenic technique, which uses simultaneous registration of heat and charge [26,27] or heat and light signals [28–30]. In Refs. [29,30] calcium tungstate crystals ( $\text{CaWO}_4$ ) are discussed as promising material for such a kind of dark matter detector. However, radioactive contamination of  $\text{CaWO}_4$  crystals used in Refs. [29,30], as well as investigated in Ref. [31], is too high for low counting measurements.<sup>1</sup>

The purpose of our work was investigation of scintillation properties and radioactive contamina-

tion of zinc tungstate ( $\text{ZnWO}_4$ ) crystals as possible detectors for the double beta decay and dark matter experiments.

## 2. Measurements and results

### 2.1. Light output and energy resolution of the $\text{ZnWO}_4$ scintillators

Three clear, slightly colored  $\text{ZnWO}_4$  crystals ( $\varnothing 14 \times 4$  mm,  $\varnothing 14 \times 7$  mm and  $\varnothing 13 \times 28$  mm) were used in our studies. The crystals were fabricated from monocrystals grown by the Czochralski method. The main properties of  $\text{ZnWO}_4$  scintillators are presented in Table 1, where characteristics of calcium and cadmium tungstates are given for comparison.

Scintillation characteristics of zinc tungstate crystals have been studied in Refs. [33–36]. Light yield of  $\text{ZnWO}_4$  was measured in Ref. [35] with the help of silicon photodiodes as 9300 photons/MeV (which is  $\approx 23\%$  of  $\text{NaI(Tl)}$  light yield). We have estimated the value of the photoelectron yield of the  $\text{ZnWO}_4$  in measurements with two scintillators:  $\text{ZnWO}_4$   $\varnothing 14 \times 7$  mm and standard  $\text{NaI(Tl)}$   $\varnothing 40 \times 40$  mm. The crystals were coupled to the PMT (EMI D724KFLB) with the bialkali RbCs photocathode. The  $\text{ZnWO}_4$  detector was wrapped by PTFE reflector tape. The relative photoelectron yield of  $\text{ZnWO}_4$  was determined as 13% of that of  $\text{NaI(Tl)}$ .

The energy resolution of  $\text{ZnWO}_4$  crystals for 662 keV  $\gamma$  rays ( $^{137}\text{Cs}$ ) has been reported as FWHM = 13% [34] and FWHM = 11.5% [36]. In the present work the energy resolution FWHM = 11.0% for 662 keV  $\gamma$  line of  $^{137}\text{Cs}$  was measured with the  $\text{ZnWO}_4$   $\varnothing 14 \times 7$  mm crystal. The crystal was wrapped by PTFE reflector tape and optically coupled to 3" photomultiplier (PMT) Philips XP2412. Taking into account slow decay of  $\text{ZnWO}_4$  scintillation, the 24  $\mu\text{s}$  shaping time of spectroscopy amplifier was set.

A substantial improvement of light collection ( $\approx 40\%$ ) and energy resolution was achieved by placing the crystal in liquid (silicone oil with index of refraction  $\approx 1.5$ ). The crystal was fixed in center of the teflon container  $\varnothing 70 \times 90$  mm and viewed

<sup>1</sup>See, however, Ref. [32].

Table 1  
Properties of ZnWO<sub>4</sub>, CaWO<sub>4</sub> and CdWO<sub>4</sub> crystal scintillators

	ZnWO <sub>4</sub>	CaWO <sub>4</sub>	CdWO <sub>4</sub>
Density (g/cm <sup>3</sup> )	7.8	6.1	8.0
Melting point (°C)	1200	1570–1650	1325
Structural type	Wolframite	Sheelite	Wolframite
Cleavage plane	Marked (010)	Weak (101)	Marked (010)
Hardness (T)	4–4.5	4.5–5	4–4.5
Wavelength of emission maximum (nm)	480	420–440	480
Refractive index	2.1–2.2	1.94	2.2–2.3
Effective average decay time* (μs)	24	8	13
Photoelectron yield [% of NaI(Tl)]*	13%	18%	20%

\*For  $\gamma$  rays, at room temperature.

by two PMTs XP2412. Fig. 1(a) demonstrates the energy spectra of <sup>137</sup>Cs and <sup>60</sup>Co obtained in such a way with the  $\varnothing 14 \times 7$  mm ZnWO<sub>4</sub> scintillation crystal. For the first time the energy resolution 9.1% and 6% was measured with ZnWO<sub>4</sub> crystal scintillator for 662 and 1333 keV  $\gamma$  lines, respectively. Furthermore, the resolution 11.3% for the 662 keV  $\gamma$  line was obtained with the larger crystal  $\varnothing 13 \times 28$  mm in the same measurement conditions.

Fig. 1(b) shows the energy spectra of <sup>241</sup>Am and <sup>55</sup>Fe low energy gamma and X-ray lines measured with the ZnWO<sub>4</sub> scintillator  $\varnothing 14 \times 4$  mm (the crystal was wrapped by PTFE reflector tape and optically coupled to the PMT XP2412). The 6 keV peak of <sup>55</sup>Fe source is still resolved from the PMT noise.

## 2.2. $\alpha/\beta$ ratio

The  $\alpha/\beta$  ratio<sup>2</sup> was measured (in the energy range of 1.0–5.3 MeV) with the help of the collimated beam of  $\alpha$  particles from an <sup>241</sup>Am source and using various sets of thin mylar films as absorbers. The energies of  $\alpha$  particles were determined with the help of a surface-barrier detector (see for details [37]). The ZnWO<sub>4</sub> crystal was irradiated in the directions perpendicular to

(010), (001) and (100) crystal planes. The dependence of the  $\alpha/\beta$  ratio on energy and direction of  $\alpha$  beam relatively to the crystal planes (see Fig. 2) is similar to that observed with CdWO<sub>4</sub> scintillators [37]. As the quenching of the scintillation light caused by  $\alpha$  particles (in comparison with electrons) is due to the higher ionization density of  $\alpha$  particles, such a behaviour of the  $\alpha/\beta$  ratio can be explained by the energy dependence of ionization density of  $\alpha$  particles [38].

## 2.3. Pulse shape discrimination

The time characteristics of ZnWO<sub>4</sub> scintillators were studied as described in Refs. [39,37] with the help of a transient digitizer based on the 12 bit ADC (AD9022) operated at the sample rate of 20 MS/s. The scintillator was irradiated by  $\approx 4.6$  MeV  $\alpha$  particles in the direction perpendicular to the (010) crystal plane. Shapes of the light pulses produced by  $\alpha$  particles and  $\gamma$  rays are depicted in Fig. 3. Fit of the pulses by the function:  $f(t) = \sum A_i / (\tau_i - \tau_0) \times (e^{-t/\tau_i} - e^{-t/\tau_0})$ ,  $t > 0$ , where  $A_i$  are intensities (in percentage of the total pulse intensity),  $\tau_i$  are decay constants for different light emission components,  $\tau_0$  is integration constant of electronics ( $\approx 0.2 \mu\text{s}$ ), gives three decay components  $\tau_i \approx 0.7$ ,  $\approx 7$  and  $\approx 25 \mu\text{s}$  with different amplitudes for  $\gamma$  rays and  $\alpha$  particles (see Table 2). The value of the slow decay component is in agreement with the result of  $25 \mu\text{s}$  obtained in Ref. [34], while  $0.7$  and  $7 \mu\text{s}$  decay time constants were identified at the first time. We were not able

<sup>2</sup>The  $\alpha/\beta$  ratio is defined as ratio of  $\alpha$  peak position in the energy scale measured with  $\gamma$  sources to the energy of  $\alpha$  particles. Because  $\gamma$  quanta interact with detector by  $\beta$  particles, we use more convenient term “ $\alpha/\beta$  ratio”.

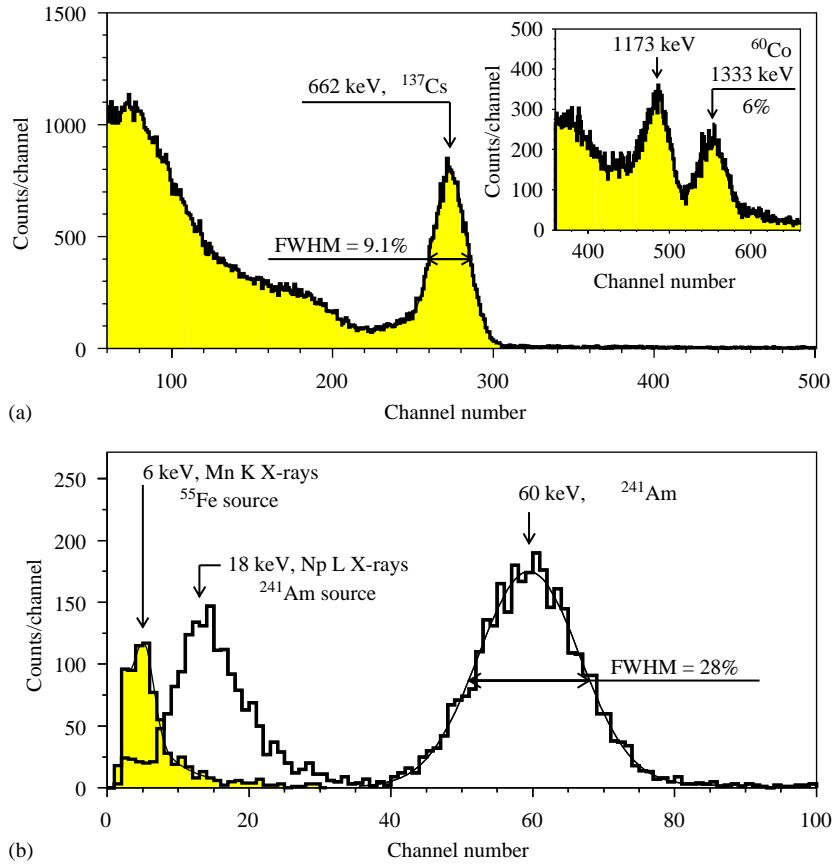


Fig. 1. (a) Energy spectra of  $^{137}\text{Cs}$  and  $^{60}\text{Co}$  (Inset)  $\gamma$  rays measured with  $\text{ZnWO}_4$  scintillation crystal  $\varnothing 14 \times 7$  mm located in liquid and viewed by two distant PMTs. (b) Energy spectra of  $^{241}\text{Am}$  and  $^{55}\text{Fe}$  low energy gamma/X-rays measured by  $\text{ZnWO}_4$  scintillation crystal ( $\varnothing 14 \times 4$  mm).

to measure the  $0.1 \mu\text{s}$  decay component reported in Ref. [34], because of the not enough fast digitizer used in our measurements.

The difference of the pulse shapes allows to discriminate  $\gamma(\beta)$  events from those of  $\alpha$  particles. For this purpose we used the optimal filter method proposed in Ref. [40], which was successfully applied to  $\text{CdWO}_4$  scintillators [39]. To obtain the numerical characteristic of scintillation signal, so-called shape indicator (SI), the following procedure was applied for each pulse:  $\text{SI} = \sum f(t_k) \times P(t_k) / \sum f(t_k)$ , where the sum is over time channels  $k$ , starting from the origin of pulse and up to  $90 \mu\text{s}$ ,  $f(t_k)$  is the digitized amplitude (at the time  $t_k$ ) of a given signal. The

weight function  $P(t)$  is defined as:  $P(t) = \{\bar{f}_\alpha(t) - \bar{f}_\gamma(t)\} / \{\bar{f}_\alpha(t) + \bar{f}_\gamma(t)\}$ , where  $\bar{f}_\alpha(t)$  and  $\bar{f}_\gamma(t)$  are the reference pulse shapes for  $\alpha$  particles and  $\gamma$  quanta. Clear discrimination between  $\alpha$  particles and  $\gamma$  rays ( $\beta$  particles) was achieved using this approach, as one can see in inset of Fig. 4 where the shape indicator distributions measured by the  $\text{ZnWO}_4$  scintillation crystal with  $\alpha$  particles ( $E_\alpha \approx 5.3 \text{ MeV}$ ) and  $\gamma$  quanta ( $\approx 1 \text{ MeV}$ ) are shown. As a measure of the discrimination ability, the following relation can be used:  $m_{\text{PSA}} = |\text{SI}_\alpha - \text{SI}_\gamma| / \sqrt{\sigma_\alpha^2 + \sigma_\gamma^2}$ , where  $\text{SI}_\alpha$  and  $\text{SI}_\gamma$  are mean SI values of  $\alpha$  particles and  $\gamma$  quanta distributions (which are well described by Gaussian functions),  $\sigma_\alpha$  and  $\sigma_\gamma$ —corresponding

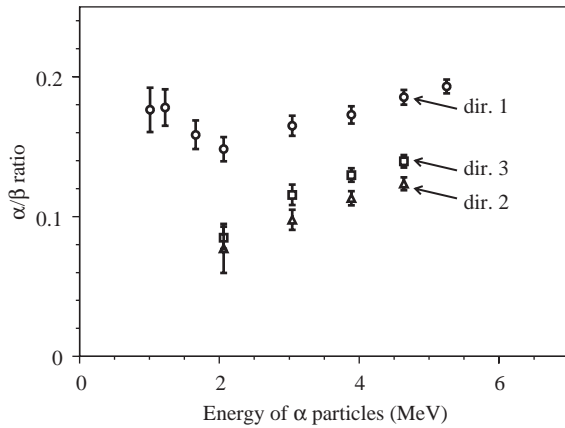


Fig. 2. The dependence of the  $\alpha/\beta$  ratio on energy of  $\alpha$  particles measured with  $\text{ZnWO}_4$  scintillator. The  $\text{ZnWO}_4$  crystal  $\varnothing 14 \times 7$  mm was irradiated in the directions perpendicular to (010), (001) and (100) crystal planes (directions 1, 2 and 3, respectively).

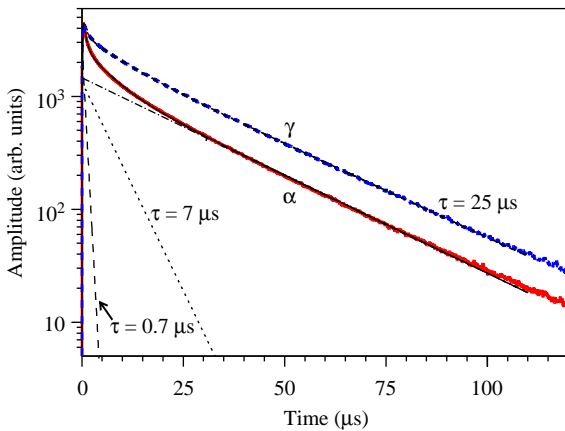


Fig. 3. Decay of scintillation in  $\text{ZnWO}_4$  for  $\gamma$  rays and  $\alpha$  particles (5 thousand forms of  $\gamma$  and  $\alpha$  signals were added) and their fit by three components with  $\tau_i \approx 0.7, \approx 7$  and  $\approx 25 \mu\text{s}$ .

Table 2  
Decay times of  $\text{ZnWO}_4$  scintillators for  $\gamma$  quanta and  $\alpha$  particles

Type of irradiation	Decay constants, $\mu\text{s}$		
	$\tau_1$ ( $A_1$ )	$\tau_2$ ( $A_2$ )	$\tau_3$ ( $A_3$ )
$\gamma$ ray	0.7 (2%)	7.5 (9%)	25.9 (89%)
$\alpha$ particles	0.7 (4%)	5.6 (16%)	24.8 (80%)

The decay constants and their intensities (in percentage of the total intensity) are denoted as  $\tau_i$  and  $A_i$ , respectively.

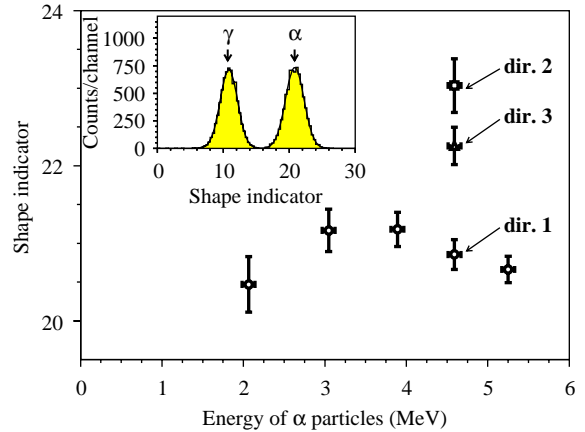


Fig. 4. Dependence of the shape indicator (see text) on the energy and directions of  $\alpha$  particles relatively to the main (010), (001) and (100) crystal planes of  $\text{ZnWO}_4$  (directions 1, 2 and 3, respectively). (Inset) The shape indicator distributions measured by  $\text{ZnWO}_4$  detector with 5.3 MeV  $\alpha$  particles and  $\approx 1$  MeV  $\gamma$  quanta.

standard deviations. For the distributions presented in inset of Fig. 4, parameter  $m_{\text{PSA}} = 5.2$ .

The energy dependence of the SI was studied with the  $\varnothing 14 \times 7$  mm  $\text{ZnWO}_4$  crystal in the 2–5.3 MeV region for  $\alpha$  particles and 0.1–2.6 MeV for  $\gamma$  quanta. No dependence of the SI on the energy of  $\gamma$  quanta was observed. The measured dependence of the SI on energy and direction of irradiation by  $\alpha$  particles (see Fig. 4) is similar to that observed with  $\text{CdWO}_4$  scintillators [37].

#### 2.4. Radioactive contamination

Radioactive contamination of the  $\text{ZnWO}_4$  crystal ( $\varnothing 14 \times 4$  mm, mass of 4.5 g) was measured in a low background set-up installed in the Solotvina Underground Laboratory built in a salt mine 430 m underground ( $\approx 1000$  m of water equivalent) [41]. In the set-up the  $\text{ZnWO}_4$  scintillation crystal was viewed by the 3" PMT (FEU-137) through the high pure quartz light-guide 4.9 cm in diameter and 25 cm long. The detector was surrounded by a passive shield made of plexiglas (6–13 cm), high purity copper (thickness 3–6 cm) and lead (15 cm).

The event-by-event data acquisition records information on the amplitude (energy) and arrival time of each detector event. The energy resolution of the detector (FWHM) for  $\gamma$  lines with the energies 60 keV ( $^{241}\text{Am}$ ), 570 keV and 1064 keV ( $^{207}\text{Bi}$ ) was measured as 37%, 15% and 10%, respectively. These data can be fitted by the function:  $\text{FWHM}_\gamma = -8.5 + \sqrt{16 \cdot E_\gamma}$ , where  $\text{FWHM}_\gamma$  and the energy of  $\gamma$  quanta  $E_\gamma$  are in keV.

The energy spectrum measured with the  $\text{ZnWO}_4$  crystal during 429 h in the low background set-up is presented in Fig. 5. The spectra of  $\text{CaWO}_4$  and  $\text{CdWO}_4$  scintillators measured in similar conditions are given for comparison (the spectra are normalized by their measurement times and detector masses). The background of the  $\text{ZnWO}_4$  detector is substantially lower than that of the  $\text{CaWO}_4$  and is comparable with that of the  $\text{CdWO}_4$  above  $\approx 0.5$  MeV. Note, that below 0.5 MeV the counting rate of the  $\text{ZnWO}_4$  detector is one order of magnitude lower than that of  $\text{CdWO}_4$ . Obviously, it is due to presence in the  $\text{CdWO}_4$  crystals of the  $\beta$  active  $^{113}\text{Cd}$  isotope (natural abundance of  $\approx 12\%$ ).

The spectrum of the  $\text{ZnWO}_4$  detector was simulated with the GEANT4 package [42]. Initial

kinematics of particles emitted in  $\alpha$  and  $\beta$  decays of nuclei was generated with the DECAY event generator [43]. The background is caused mainly by  $\gamma$  quanta from the PMT. In the spectrum there are no peculiarities which could be referred to the internal trace radioactivity. Therefore, only limits on contaminations of this crystal by nuclides from U–Th families as well as by  $^{40}\text{K}$ ,  $^{90}\text{Sr}$ – $^{90}\text{Y}$ ,  $^{137}\text{Cs}$ , and  $^{147}\text{Sm}$  were set on the basis of the experimental data. With this aim the spectrum was fitted in different energy intervals by simple model composed of an exponential function (to describe external  $\gamma$  rays) and background components searched for (simulated with the GEANT4 package). Because equilibrium of U–Th families in crystals is expected to be broken, different part of the families were considered separately. Results of these estimations are presented in Table 3.

More sensitive limits on radioactive impurities associated with the daughters of  $^{232}\text{Th}$ ,  $^{235}\text{U}$  and  $^{238}\text{U}$  were obtained with the help of the time-amplitude analysis described in detail in Refs. [46,11]. For example, the fast sequence of

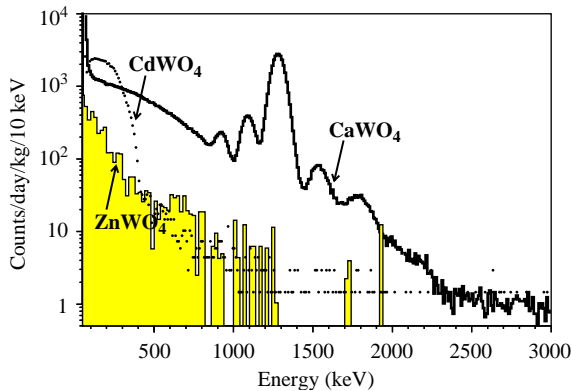


Fig. 5. Energy spectra of  $\text{ZnWO}_4$  (4.5 g, 429 h),  $\text{CaWO}_4$  (189 g, 1734 h), and  $\text{CdWO}_4$  (448 g, 37 h) scintillation crystals measured in the low background set-up. The  $\text{CaWO}_4$  crystal is considerably polluted by radionuclides from U–Th chains (see for details [31]). Beta decay of  $^{113}\text{Cd}$  ( $Q_\beta = 316$  keV,  $T_{1/2} = 7.7 \times 10^{15}$  years) dominates in the low energy part of the  $\text{CdWO}_4$  spectrum. The background of the  $\text{ZnWO}_4$  detector is caused mainly by external  $\gamma$  rays.

Table 3  
Radioactive contaminations in  $\text{ZnWO}_4$ ,  $\text{CaWO}_4$  and  $\text{CdWO}_4$  crystal scintillators

Chain	Source	Activity (mBq/kg)		
		$\text{ZnWO}_4$	$\text{CaWO}_4$ [31]	$\text{CdWO}_4$ [44,45,8,9]
$^{232}\text{Th}$	$^{232}\text{Th}$	$\leq 3.3$	0.69(10)	0.053(5)
	$^{228}\text{Th}$	$\leq 0.2$	0.6(2)	$\leq 0.004 - 0.039(2)$
$^{235}\text{U}$	$^{227}\text{Ac}$	$\leq 0.2$	1.6(3)	0.0014(9)
$^{238}\text{U}$	$^{238}\text{U}$	$\leq 3.2$	14.0(5)	$\leq 0.6$
	$^{230}\text{Th}$	$\leq 4.5$	—	$\leq 0.5$
	$^{226}\text{Ra}$	$\leq 0.4$	5.6(5)	$\leq 0.004$
	$^{210}\text{Pb}$	$\leq 1$	$\leq 430$	$\leq 0.4$
	$^{210}\text{Po}$	—	291(5)	—
	$^{206}\text{Pb}$	—	—	—
	$^{40}\text{K}$	$\leq 12$	$\leq 12$	0.3(1)
	$^{90}\text{Sr}$	$\leq 1.2$	$\leq 70$	$\leq 0.2$
	$^{113}\text{Cd}$	—	—	580(20)
	$^{113m}\text{Cd}$	—	—	1–30
	$^{137}\text{Cs}$	$\leq 20$	$\leq 0.8$	$\leq 0.3 - 0.43(6)$
	$^{147}\text{Sm}$	$\leq 1.8$	0.49(4)	$\leq 0.04$

Table 4  
Half-life limits on  $2\beta$  processes in zinc and tungsten isotopes.

Transition $\Delta M$ in keV $\delta$ in %	Decay channel	Decay mode	Experimental $T_{1/2}$ limit (years)	
			Present work 90% (68%) CL	Previous limits
$^{64}\text{Zn} \rightarrow ^{64}\text{Ni}$ 1096.4 (0.9) 48.63 (0.60)	$2\varepsilon$	0v	$0.7 (1.0) \times 10^{18}$	$8 \times 10^{15}$ [49]
	$\varepsilon\beta^+$	2v	$4.3 (8.9) \times 10^{18}$	$2.3 \times 10^{18}$ (68% CL) [50]
	$\varepsilon\beta^+$	0v	$2.4 (3.6) \times 10^{18}$	$2.3 \times 10^{18}$ (68% CL) [50] $T_{1/2} = (1.1 \pm 0.9) \times 10^{19}$ years [51]
$^{70}\text{Zn} \rightarrow ^{70}\text{Ge}$ 1000.9 (3.4) 0.62 (0.03)	$2\beta^-$	2v	$1.3 (2.1) \times 10^{16}$	—
	$2\beta^-$	0v	$0.7 (1.4) \times 10^{18}$	$1.3 \times 10^{16}$ (90% CL) [52]
$^{180}\text{W} \rightarrow ^{180}\text{Hf}$ 146 (5) 0.12 (0.01)	2K	2v	$0.7 (0.8) \times 10^{16}$	$0.7 (0.8) \times 10^{17}$ 90% (68%) CL [9]
	$2\varepsilon$	0v	$0.9 (1.1) \times 10^{16}$	$0.9 (1.3) \times 10^{17}$ 90% (68%) CL [9]
$^{186}\text{W} \rightarrow ^{186}\text{Os}$ 488.0 (1.7) 28.43 (0.19)	$2\beta^-$	2v	$1.4 (2.5) \times 10^{18}$	$3.7 (5.3) \times 10^{18}$ 90% (68%) CL [9]
	$2\beta^-$	0v	$1.1 (1.7) \times 10^{19}$	$1.1 (2.1) \times 10^{21}$ 90% (68%) CL [9]

Mass difference [47] and isotopic abundance [48] are denoted as  $\Delta M$  and  $\delta$ , respectively.

two  $\alpha$  decays from the  $^{232}\text{Th}$  family was searched for:  $^{220}\text{Rn}$  ( $Q_\alpha = 6.41$  MeV,  $T_{1/2} = 55.6$  s)  $\rightarrow$   $^{216}\text{Po}$  ( $Q_\alpha = 6.91$  MeV,  $T_{1/2} = 0.145$  s)  $\rightarrow$   $^{212}\text{Pb}$  (which are in equilibrium with  $^{228}\text{Th}$ ). No events were selected by using this method and the limit  $\leq 0.2$  mBq/kg on the activity of  $^{228}\text{Th}$  was set. In the same way, the absence of the fast sequences  $^{214}\text{Bi}$  ( $Q_\beta = 3.27$  MeV,  $T_{1/2} = 19.9$  m)  $\rightarrow$   $^{214}\text{Po}$  ( $Q_\alpha = 7.83$  MeV,  $T_{1/2} = 164$   $\mu$ s)  $\rightarrow$   $^{210}\text{Pb}$  from  $^{238}\text{U}$  family, and  $^{219}\text{Rn}$  ( $Q_\alpha = 6.95$  MeV,  $T_{1/2} = 3.96$  s)  $\rightarrow$   $^{215}\text{Po}$  ( $Q_\alpha = 7.53$  MeV,  $T_{1/2} = 1.78$  ms)  $\rightarrow$   $^{211}\text{Pb}$  from  $^{235}\text{U}$  chain leads to the following limits:  $^{226}\text{Ra} \leq 0.4$  mBq/kg, and  $^{227}\text{Ac} \leq 0.2$  mBq/kg.

### 3. Discussion

#### 3.1. Search for $2\beta$ processes in zinc and tungsten

Double  $\beta$  decay of two zinc ( $^{64}\text{Zn}$  and  $^{70}\text{Zn}$ ) and two tungsten ( $^{180}\text{W}$  and  $^{186}\text{W}$ ) isotopes can be studied with the help of  $\text{ZnWO}_4$  detector. Their

mass differences, isotopic abundances, possible decay channels are listed in Table 4. We performed preliminary investigation to check a possibility of such experiments using the data of the low background measurements with the  $\text{ZnWO}_4$  scintillator  $\varnothing 14 \times 4$  mm.

In the energy spectrum accumulated with the  $\text{ZnWO}_4$  crystal (see Fig. 6) there are no peculiarities which can be attributed to  $2\beta$  processes in the mentioned zinc or tungsten isotopes.<sup>3</sup> Therefore only lower half-life limits can be set according to formula:  $\lim T_{1/2} = N \cdot \eta \cdot t \cdot \ln 2 / \lim S$ , where  $N$  is the number of potentially  $2\beta$  unstable nuclei,  $\eta$  is the detection efficiency,  $t$  is the measuring time and  $\lim S$  is the number of events of the effect searched for which can be excluded with a given confidence level (CL).

<sup>3</sup>The response functions of the  $\text{ZnWO}_4$  detector expected for the different channels and modes of  $2\beta$  processes in zinc and tungsten were simulated with the help of the DECAY [43] and GEANT4 [42] codes.

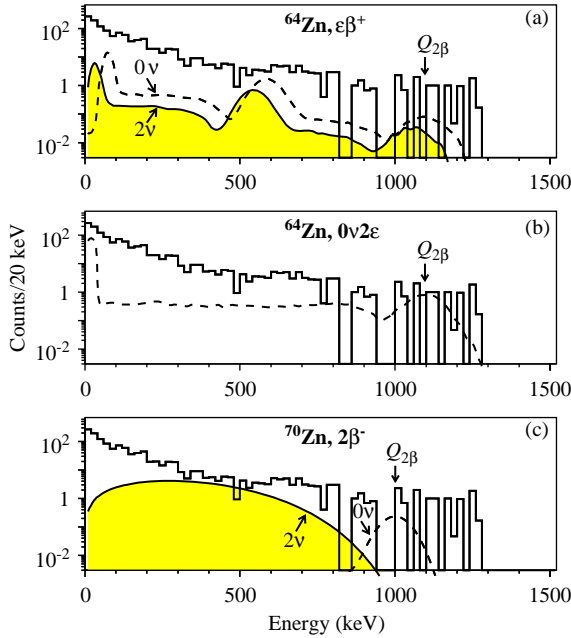


Fig. 6. The background energy spectrum of  $\text{ZnWO}_4$  scintillation crystal (4.5 g of mass, 429 h measurements in the Solotvina Underground Laboratory) together with the excluded at 68% CL distributions for  $\varepsilon\beta^+$  (a) and  $0\nu 2\varepsilon$  (b) processes in  $^{64}\text{Zn}$ . (c) The excluded at 68% CL distributions for the  $2\beta^-$  decays of  $^{70}\text{Zn}$ .

### 3.1.1. $^{64}\text{Zn}$ ( $\varepsilon\beta^+$ )

The energy of the first excited level of  $^{64}\text{Ni}$  (1346 keV) is higher than the  $Q_{2\beta}$  value of  $^{64}\text{Zn}$ , therefore transitions only to the ground state of  $^{64}\text{Ni}$  are allowed. To estimate the value of  $\lim S$  for the two neutrino mode of electron capture in  $^{64}\text{Zn}$  with positron emission ( $2\nu\varepsilon\beta^+$ ), the experimental spectrum was fitted in the energy interval 380–800 keV. The simple model including the effect searched for and an exponential function (to describe the background) was chosen. The least squares fit ( $\chi^2/n.d.f. = 21.5/19 = 1.1$ ) gives total area of the effect  $-15 \pm 29$  counts which corresponds (in accordance with the Particle Data Group recommendations [53]) to  $\lim S = 34(16)$  counts at 90% (68%) CL. Taking into account  $\approx 100\%$  registration efficiency and number of  $^{64}\text{Zn}$  nuclei in the crystal ( $N = 4.21 \times 10^{21}$ ), one can calculate the half-

life limit:

$$T_{1/2}^{2\nu\varepsilon\beta^+} \geq 4.2(8.9) \times 10^{18} \text{ years at 90\% (68\%) CL.}$$

In the same way the half-life bound on the neutrinoless mode was set:

$$T_{1/2}^{0\nu\varepsilon\beta^+} \geq 2.4(3.6) \times 10^{18} \text{ years at 90\% (68\%) CL.}$$

The experimental spectrum of the  $\text{ZnWO}_4$  crystal in the energy interval 50–1500 keV is presented in Fig. 6(a) together with excluded at 68% CL distributions of the  $2\nu$  and  $0\nu\varepsilon\beta^+$  decay of  $^{64}\text{Zn}$ . Despite the very little detector mass and short exposure used in the present work, the obtained limits are higher than those reported before ( $T_{1/2} \geq 2.3 \times 10^{18}$  years at 68% CL for  $2\nu$  and  $0\nu$  processes [50]).

Recently, an experimental observation of the  $\varepsilon\beta^+$  decay of  $^{64}\text{Zn}$  with  $T_{1/2}^{(0\nu+2\nu)\varepsilon\beta^+} = (1.1 \pm 0.9) \times 10^{19}$  years was claimed in [51]. A  $\varnothing 7.6 \times 7.6$  cm NaI(Tl) scintillation and a 25% efficiency HPGe detector, operated in coincidence, were used in the experiment. The excess of  $\approx 85$  events in the 511 keV peak was observed with zinc sample (mass of 350 g, 392 h of exposure), while no effect was detected without sample or with copper (iron) blanks. Unfortunately, possible radioactive contamination of the zinc sample (which could give the observed excess of events) and of the Cu and Fe blanks were not discussed in Ref. [51], and, to our knowledge, no further experiments were carried out to prove or elaborate this result.

We have estimated the sensitivity of an experiment with about one kg  $\text{ZnWO}_4$  crystal<sup>4</sup> ( $\approx 10^{24}$  of  $^{64}\text{Zn}$  nuclei) to  $\varepsilon\beta^+$  decay of  $^{64}\text{Zn}$ . As it was shown by the GEANT4 simulation, the registration efficiency in the high energy part of the expected  $\varepsilon\beta^+$  distributions will be substantially increased (at least by an order of magnitude). Supposing additional decrease of background by a factor of  $\approx 5$  (due to larger detector, improvement of the set-up, and time-amplitude and pulse shape analyses), we expect to reach after  $\approx 1$  year of exposure the sensitivity (in terms of the half-life limit) of  $\approx 5 \times 10^{21}$  years both for the  $0\nu$  and  $2\nu$

<sup>4</sup>Even larger zinc tungstate crystals ( $\varnothing 60 \times 150$  mm, that is of  $\approx 3$  kg) can be produced [33].



modes. Thus, the  $2\nu\varepsilon\beta^+$  decay of  $^{64}\text{Zn}$  at the level of  $10^{20}$  years could be surely observed, proving or disproving the result of Ref. [51]. It should be noted, that the  $0\nu$  and  $2\nu$  modes of the  $\varepsilon\beta^+$  process in  $^{64}\text{Zn}$  can be distinguished with a  $\text{ZnWO}_4$  detector, while it is impossible to do in experiments similar to Ref. [51], where external zinc sample was used.

### 3.1.2. $^{64}\text{Zn}$ ( $2\varepsilon$ )

For the  $2\nu$  double electron capture in  $^{64}\text{Zn}$  from K-shell the total energy released in a detector is equal to  $2E_K = 16.7\text{ keV}$  (where  $E_K = 8.3\text{ keV}$  is the binding energy of electrons on K-shell of nickel atoms). Detection of such a little energy deposit requires rather low energy threshold. In our measurements the energy threshold for acquisition was not enough low to search for  $2\nu 2K$  decay in  $^{64}\text{Zn}$ . However, as one can see on Fig. 1(b), X-rays with the energy of a few keV can be resolved from PMT noise.

At the same time, the neutrinoless mode of  $2\varepsilon$  process in  $^{64}\text{Zn}$  can be searched for using the existing data. In such a process all available energy has to be transferred to  $\gamma$  quanta, conversion electrons, X-rays or Auger electrons. Corresponding simulated distribution is shown in Fig. 6(b) where we supposed transfer of energy to one  $\gamma$  quantum, the most disadvantageous process with the point of view of efficiency of detection. The maximum likelihood fit in the energy interval 400–1300 keV gives  $59 \pm 86$  counts for the effect searched for, which leads to the half-life limit:

$$T_{1/2}^{0\nu 2K} \geq 0.7(1.0) \times 10^{18} \text{ years at 90\% (68\%) CL.}$$

This limit is higher than that obtained in Ref. [49].

It should be stressed, that  $^{64}\text{Zn}$  is one of only few potentially  $2\varepsilon/\varepsilon\beta^+$  unstable nuclides with rather high natural abundance (see, for instance, review [4]). Therefore large-scale experiment to search for double beta processes in  $^{64}\text{Zn}$  can be realized without using of high cost enriched isotopes.

### 3.1.3. $^{70}\text{Zn}$ ( $2\beta^-$ )

The peak at 1001 keV with energy resolution  $\text{FWHM} = 118\text{ keV}$  is expected in the spectrum of

the  $\text{ZnWO}_4$  detector for the  $0\nu 2\beta$  decay of  $^{70}\text{Zn}$ . Number of  $^{70}\text{Zn}$  nuclei in the crystal is  $5.4 \times 10^{19}$ , registration efficiency  $\eta \approx 100\%$ . Maximum likelihood fit of the background spectra in the energy range 0.7–1.3 MeV gives  $-0.6 \pm 1.9$  counts for the area of the effect searched for, which corresponds (again using the recommendations [53]) to  $\text{lim } S = 2.6(1.3)$  counts at 90% (68%) CL. It allows us to restrict the half-life of  $^{70}\text{Zn}$  relatively to the  $0\nu 2\beta$  decay:

$$T_{1/2}^{0\nu 2\beta} \geq 0.7(1.4) \times 10^{18} \text{ years at 90\% (68\%) CL.}$$

Similarly, the lower half-life limit on the  $2\nu 2\beta$  decay of  $^{70}\text{Zn}$  decay was established as:

$$T_{1/2}^{2\nu 2\beta} \geq 1.3(2.1) \times 10^{16} \text{ years at 90\% (68\%) CL.}$$

The excluded at 68% CL distributions corresponding to  $2\beta$  decays of  $^{70}\text{Zn}$  are presented in Fig. 6(c).

Despite modest level of these results, the limit on the neutrinoless mode of  $2\beta$  decay of  $^{70}\text{Zn}$  is higher than that obtained in recent experiment [52] while the  $2\nu$  mode is elaborated for the first time.

### 3.1.4. $^{180}\text{W}$ and $^{186}\text{W}$

We have also estimated the half-life limits on the  $2\beta$  decay of  $^{180}\text{W}$  and  $^{186}\text{W}$  on the basis of the measurements with the  $\text{ZnWO}_4$  crystal. All the limits (see Table 4) are lower than those set earlier with 330 g  $\text{CdWO}_4$  detector operated during much longer time (692 h for  $^{180}\text{W}$  and 13316 h for  $^{186}\text{W}$ ) [12,9]. However, the advantage of the  $\text{ZnWO}_4$  detector (as compared with  $\text{CdWO}_4$ ) is absence of the  $\beta$  active  $^{113}\text{Cd}$  and  $2\nu 2\beta$  active  $^{116}\text{Cd}$  isotopes. As a result, background of the  $\text{ZnWO}_4$  detector in the energy interval of interest is much lower. Therefore sensitivity to search for the double beta processes in  $^{180}\text{W}$  and  $^{186}\text{W}$  could be improved with a larger  $\text{ZnWO}_4$  detector.

### 3.2. $\alpha$ decay of $^{180}\text{W}$

It should be also mentioned a potentiality of  $\text{ZnWO}_4$  detector (scintillator or bolometer) to measure alpha decay of  $^{180}\text{W}$ , indication of which (with the half-life  $\approx 10^{18}$  years) has been obtained in the low background experiment with  $\text{CdWO}_4$  crystal scintillators [37] and confirmed recently in

the measurements with  $\text{CaWO}_4$  as scintillator [31] and bolometer [54].

### 3.3. $\text{ZnWO}_4$ as detector for the dark matter particles search

The  $\text{CaWO}_4$  crystals are promising material for a dark matter detector. Powerful background suppression was realized in Refs. [29,30] due to simultaneous registration of heat and light signals. However, radioactive contaminations of the crystal used in Refs. [29,30], as well as investigated in work [31], are rather high. Radioactive contamination of the  $\text{ZnWO}_4$  crystal is essentially lower than that of  $\text{CaWO}_4$ . Although there are no data about performance of  $\text{ZnWO}_4$  crystals as low temperature particle detectors,  $\text{ZnWO}_4$  is expected to be an applicable material for bolometric technique taking into account the encouraging results obtained with physically analogous  $\text{CdWO}_4$  [55] and  $\text{CaWO}_4$  [29,30] crystals.

If so,  $\text{ZnWO}_4$  crystals could provide an interesting possibility to search for spin-dependent inelastic scattering of WIMP with excitation of low energy nuclear levels (see Table 5 where nuclides with nonzero spin presented in  $\text{ZnWO}_4$  crystals are listed). Identification of such “mixed” (nuclear recoil plus  $\gamma$  quanta) events could be possible due to the simultaneous registration of heat and light signals. A heat/light ratio for such events would differ from “pure” nuclear recoils or  $\gamma(\beta)$  events. For example, search for spin-dependent inelastic scattering of WIMP with excitation of the  $^{67}\text{Zn}$  and/or  $^{183}\text{W}$  low-energy nuclear levels (93 and 47 keV, respectively) can be realized with  $\text{ZnWO}_4$  crystals. Detection of nuclear recoils and delayed (with the half-life 9  $\mu\text{s}$  in the case of  $^{67}\text{Zn}$ )

$\gamma$  quanta could give a strong signature for the process searched for.

In addition, the observed with  $\text{ZnWO}_4$  scintillators dependence of pulse shape on the direction of  $\alpha$  particles irradiation relative to the crystal axes (supposing that such a dependence would remain valid for nuclear recoils) could be used to detect a diurnal asymmetry of WIMP direction [13].

## 4. Conclusions

Scintillation properties of  $\text{ZnWO}_4$  crystals were studied. The energy resolution 9.1% (662 keV  $^{137}\text{Cs}$   $\gamma$  line) was obtained with  $\text{ZnWO}_4$  crystal scintillator placed in liquid and viewed by two PMTs. Shapes of scintillation signals was investigated, and clear pulse-shape discrimination for  $\gamma(\beta)$  and  $\alpha$  events was achieved. Dependences of the  $\alpha/\beta$  ratio and scintillation pulse shape on the energy of  $\alpha$  particles were measured. It was also found that the  $\alpha/\beta$  ratio and pulse shape show the dependence on direction of  $\alpha$  irradiation relatively to the main crystal planes of  $\text{ZnWO}_4$  crystal.

Radioactive contamination of  $\text{ZnWO}_4$  crystal was measured in the Solotvina Underground Laboratory. No radioactive pollution in  $\text{ZnWO}_4$  scintillator was observed. Limits on radioactive contamination in  $\text{ZnWO}_4$  crystal are on the level from tenth to a few mBq/kg which is one–two order of magnitude lower than those for  $\text{CaWO}_4$ .

Two potentially  $2\beta$  active zinc and two tungsten isotopes ( $^{64}\text{Zn}$ ,  $^{70}\text{Zn}$ ,  $^{180}\text{W}$ , and  $^{186}\text{W}$ ) were studied with the help of  $\text{ZnWO}_4$  crystal. New improved half-life limits on double beta decay in zinc isotopes were established. In particular, for the

Table 5  
Nuclides with non-zero spin present in  $\text{ZnWO}_4$  crystals (data from Ref. [56])

Nuclide	Spin, parity	Isotopic abundance (%)	First excited level	
			Energy (keV)	Life time
$^{17}\text{O}$	$5/2^+$	0.038	870.7	179 ps
$^{67}\text{Zn}$	$5/2^-$	4.1	93.3	9.16 $\mu\text{s}$
$^{183}\text{W}$	$1/2^-$	14.3	46.5	0.188 ns

$2\nu\beta\beta^+$  decay of  $^{64}\text{Zn}$  the half-life limit was set as  $T_{1/2}^{2\nu\beta\beta^+} \geq 8.9 \times 10^{18}$  years at 68% CL.

Due to a low level of radioactive contamination,  $\text{ZnWO}_4$  crystals seem to be encouraging material for the dark matter experiments.  $\text{ZnWO}_4$  crystals could provide a possibility to search for spin-dependent inelastic scattering of WIMP with excitation of low energy nuclear levels. Most interesting targets are  $^{67}\text{Zn}$  and  $^{183}\text{W}$ .

A strong signature can be used to search for spin-dependent inelastic scattering of WIMP on nuclei with nonzero spin (which are present in  $\text{ZnWO}_4$  crystals), via registration of nuclear recoils and delayed  $\gamma$  quanta. Due to dependence of  $\text{ZnWO}_4$  scintillation pulse shape on direction of irradiation by high ionizing particles, there is *in principle* a possibility to search for diurnal modulation of WIMP direction. It could be a strong signature for WIMP evidence.

## References

- [1] J.D. Vergados, Phys. Rep. 361 (2002) 1.
- [2] Yu.G. Zdesenko, Rev. Mod. Phys. 74 (2002) 663.
- [3] S.R. Elliot, P. Vogel, Ann. Rev. Nucl. Part. Sci. 52 (2002) 115.
- [4] V.I. Tretyak, Yu.G. Zdesenko, At. Data Nucl. Data Tables 61 (1995) 43;  
V.I. Tretyak, Yu.G. Zdesenko, At. Data Nucl. Data Tables 80 (2002) 83.
- [5] P. Belli, et al., Nucl. Phys. B 563 (1999) 97.
- [6] E. der Mateosian, M. Goldhaber, Phys. Rev. 146 (1966) 810.
- [7] I. Ogawa, et al., Nucl. Phys. A 730 (2004) 215.
- [8] F.A. Danevich, et al., Z. Phys. A 355 (1996) 433.
- [9] F.A. Danevich, et al., Phys. Rev. C 68 (2003) 035501.
- [10] P. Belli, et al., Nucl. Instr. and Meth. A 498 (2003) 352.
- [11] F.A. Danevich, et al., Nucl. Phys. A 694 (2001) 375.
- [12] F.A. Danevich, et al., Nucl. Phys. A 717 (2003) 129.
- [13] L. Bergstrom, Rep. Prog. Phys. 63 (2000) 793;  
L. Bergstrom, Nucl. Phys. B (Proc. Suppl.) 118 (2003) 329;  
Y. Ramachers, Nucl. Phys. B (Proc. Suppl.) 118 (2003) 341.
- [14] L. Baudis, et al., Phys. Rev. D 59 (1998) 022001;  
B. Majorovits, et al., Nucl. Instr. and Meth. A 455 (2000) 369;  
L. Baudis, et al., Phys. Rev. D 63 (2000) 022001.
- [15] A. Morales, et al., Phys. Lett. B 489 (2000) 268;  
A. Morales, et al., Phys. Lett. B 532 (2002) 8.
- [16] A.A. Klimenko, et al., JETP Lett. 67 (1998) 875.
- [17] A. Alessandrello, et al., Phys. Lett. B 408 (1997) 465;  
G. Gervasio, (CUORE collaboration), Nucl. Phys. A 663&664 (2000) 873c.
- [18] W. Ootani, et al., Phys. Lett. B 461 (1999) 371.
- [19] C. Bacci, et al., Astropart. Phys. 2 (1994) 13;  
R. Bernabei, et al., Phys. Lett. B 389 (1996) 757;  
R. Bernabei, et al., Phys. Lett. B 424 (1998) 195;  
R. Bernabei, et al., Phys. Lett. B 450 (1999) 448;  
R. Bernabei, et al., Phys. Lett. B 480 (2000) 23;  
R. Bernabei, et al., Phys. Lett. B 509 (2001) 197;  
R. Bernabei, et al., Eur. Phys. J. C 23 (2002) 61;  
R. Bernabei, et al., Riv. Nuovo. Cim. 26 (2003) 1.
- [20] M.L. Sarsa, et al., Phys. Rev. D 56 (1997) 1856.
- [21] N.J.C. Spooner, et al., Phys. Lett. B 473 (2000) 330.
- [22] G. Gerbier, et al., Astropart. Phys. 11 (1999) 287.
- [23] C. Bacci, et al., Astropart. Phys. 2 (1994) 117;  
R. Bernabei, et al., Astropart. Phys. 6 (1997) 101;  
P. Belli, et al., Nucl. Phys. B 563 (1999) 97.
- [24] I. Ogawa, et al., Nucl. Phys. A 663&664 (2000) 869c.
- [25] R. Bernabei, et al., Phys. Lett. B 436 (1998) 379.
- [26] A. Benoit, et al., Phys. Lett. B 479 (2000) 8;  
A. Benoit, et al., Phys. Lett. B 513 (2001) 15;  
A. Benoit, et al., Phys. Lett. B 545 (2002) 43.
- [27] R. Abusaidi, et al., Phys. Rev. Lett. 84 (2000) 5699;  
T. Saab, et al., Nucl. Phys. B (Proc. Suppl.) 110 (2002) 100.
- [28] C. Bobin, et al., Nucl. Instr. and Meth. A 386 (1997) 453.
- [29] M. Bravin, et al., Astropart. Phys. 12 (1999) 107.
- [30] S. Cebrian, et al., Phys. Lett. B 563 (2003) 48.
- [31] Yu.G. Zdesenko, et al., Nucl. Instr. and Meth. A 538 (2005) 657.
- [32] Yu.G. Zdesenko, et al., Astropart. Phys. 23 (2005) 249.
- [33] B.C. Grabmaier, IEEE Trans. Nucl. Sci. NS-31 (1984) 372.
- [34] Y.C. Zhu, et al., Nucl. Instr. and Meth. A 244 (1986) 579.
- [35] I. Holl, et al., IEEE Trans. Nucl. Sci. NS-35 (1988) 105.
- [36] F.A. Danevich, et al., Prib. Tekh. Eksp. 5 (1989) 80 [Instrum. Exp. Tech. 32 (1989) 1059].
- [37] F.A. Danevich, et al., Phys. Rev. C 67 (2003) 014310.
- [38] J.B. Birks, Theory and Practice of Scintillation Counting, Pergamon, London, 1964.
- [39] T. Fazzini, et al., Nucl. Instr. and Meth. A 410 (1998) 213.
- [40] E. Gatti, F. De Martini, Nuclear Electronics, vol. 2, IAEA, Vienna, 1962, pp. 265.
- [41] Yu.G. Zdesenko, et al., Proceedings of the Second International Symposium on Underground Physics, Baksan Valley, USSR, August 17–19, 1987—Moscow, Nauka, 1988, pp. 291.
- [42] S. Agostinelli, (GEANT4 Collaboration), et al., Nucl. Instr. and Meth. A 506 (2003) 250;  
<http://geant4.web.cern.ch/geant4/>.
- [43] O.A. Ponkratenko, et al., Phys. At. Nucl. 63 (2000) 1282;  
V.I. Tretyak, to be published.
- [44] A.Sh. Georgadze, et al., Prib. Tekh. Exp. 2 (1996) 45 [Instrum. Exp. Tech. 39 (1996) 191].
- [45] S.Ph. Burachas, et al., Nucl. Instr. and Meth. A 369 (1996) 164.
- [46] F.A. Danevich, et al., Phys. Lett. B 344 (1995) 72.
- [47] G. Audi, A.H. Wapstra, Nucl. Phys. A 595 (1995) 409.

- [48] K.J.R. Rosman, P.D.P. Taylor, *Pure Appl. Chem.* 70 (1998) 217.
- [49] A. Berthelot, et al., *Compt. Rend.* 236 (1953) 1769.
- [50] E.B. Norman, *Phys. Rev. C* 31 (1985) 1937.
- [51] I. Bikit, et al., *Appl. Radiat. Isot.* 46 (1995) 455.
- [52] H. Kiel, et al., *Nucl. Phys. A* 723 (2003) 499.
- [53] K. Hagiwara, et al., *Phys. Rev. D* 66 (2002) 010001.
- [54] C. Cozzini, et al., *Phys. Rev. C* 70 (2004) 064606.
- [55] A. Alessandrello, et al., *Nucl. Instr. and Meth. A* 344 (1994) 243;  
A. Alessandrello, et al., *Nucl. Phys. B (Proc. Suppl.)* 35 (1994) 394;  
E. Fiorini, *Nucl. Phys. B (Proc. Suppl.)* 110 (2002) 233.
- [56] R.B. Firestone, et al., (Eds.), *Table of Isotopes*, eighth ed., Wiley, New York, 1996.